A Unifying Framework for Correspondence-Less Shape Alignment and Its Medical Applications

Zoltan Kato

Department of Image Processing and Computer Graphics,
University of Szeged, P.O. Box 652., 6701 Szeged, Hungary
kato@inf.u-szeged.hu

Abstract. We give an overview of our general framework for registering 2D and 3D objects without correspondences. Classical solutions consist in extracting landmarks, establishing correspondences and then the aligning transformation is obtained via a complex optimization procedure. In contrast, our framework works without landmark correspondences, is independent of the magnitude of transformation, easy to implement, and has a linear time complexity. The efficiency and robustness of the method has been demonstarted using various deformations models. Herein, we will focus on medical applications.

Keywords: Registration, Shape, 3D Object, Affine transformation, Thin plate splines, Bone Fracture, Prostate, MRI, TRUS.

1 Introduction

Registration is a crucial step when images of different views or sensors of an object need to be compared or combined. Application areas include visual inspection, target tracking in video sequences, super resolution, or medical image analysis. In a general setting, one is looking for a transformation which aligns two images such that one image (called the *observation*, or moving image) becomes similar to the second one (called the *template*, or model image). When registering an image pair, first we have to characterize the possible deformations. From this point of view, registration techniques can be classified into two main categories: physical model-based and parametric or functional representation [1]. Herein, we deal with the latter representation, which typically originate from interpolation and approximation theory.

From a methodological point of view, we can differentiate *feature-based* and *area-based* methods. *Feature-based* methods [2] aim at establishing point correspondences between two images. The main drawback of these methods is the assumption of a limited deformation and high computational cost. Their main advantage is that as long as a sufficient number of point matches are available, one can usually find an optimal aligning transformation implying that feature-based algorithms are less sensitive to occlusions. *Area-based* methods [3, 4] treat the problem without attempting to detect salient objects. The drawback of this family of methods is also the high computational cost and the restricted range

A. Agrawal et al. (Eds.): IITM 2013, CCIS 276, pp. 40–52, 2013.

of distortions. In many situations, the variability of image features is so complex (*e.g.* multimodal medical images) that it is more efficient to reduce them to a binary representation and solve the registration problem in that context. Therefore binary registration (*i.e.* shape alignment) is an important problem for many complex image analysis tasks. Herein, we will present our generic framework for recovering linear [5–8] and nonlinear [9–12] deformations of 2D and 3D objects without correspondences.

For example, spline-based deformations have been commonly used to register prostate images or volumes. The interpolating Thin-plate Splines (TPS) was originally proposed by [29], which relies on a set of point correspondences between the image pairs. However, these correspondences are prone to error in real applications and therefore [13] extended the bending energy of TPS to approximation and regularization by introducing the correspondence localization error. On the other hand, we [10] proposed a generic framework for non-rigid registration which does not require explicit point correspondences. In [14], this framework has been adopted to solve multimodal registration of MRI and TRUS prostate images.

Another prominent medical application is complex bone fracture reduction which frequently requires surgical care, especially when angulation or displacement of bone fragments are large. In such situations, computer aided surgical planning is done before the actual surgery takes place, which allows to gather more information about the dislocation of the fragments and to arrange and analyze the surgical implants to be inserted. A crucial part of such a system is the relocation of bone fragments to their original anatomic position. In [9], we applied our framework to reduce pelvic fractures using 3D rigid-body transformations. In cases of single side fractures, the *template* is simply obtained by mirroring intact bones of the patient.

2 Registration Framework

Let us denote the point coordinates of the *template* and *observation* by $\mathbf{x} \in \mathbb{R}^n$ and $\mathbf{y} \in \mathbb{R}^n$ respectively. Corresponding point pairs $(\mathbf{x}, \mathbf{y})$ are related by an unknown diffeomorphism $\phi : \mathbb{R}^n \to \mathbb{R}^n$ such that

$$\mathbf{y} = \phi(\mathbf{x}) \quad \Leftrightarrow \quad \mathbf{x} = \phi^{-1}(\mathbf{y}), \tag{1}$$

where $\phi^{-1} : \mathbb{R}^n \to \mathbb{R}^n$ is the corresponding inverse transformation. Note that ϕ^{-1} always exists since a diffeomorphism is a bijective function such that both the function and its inverse have continuous mixed partial derivatives. The goal of registration is to recover the aligning transformation ϕ.

Classical approaches would establish a set of point correspondences $\{(\mathbf{x}_i, \mathbf{y}_i)\}_{i=1}^N$ and, making use of Eq. (1), define a *similarity metric* $S(\{(\mathbf{x}_i, \mathbf{y}_i)\}, \hat{\phi})$ which characterizes the geometric alignment of the point pairs $\{(\mathbf{x}_i, \hat{\phi}(\mathbf{y}_i))\}$ achieved by a particular transformation $\hat{\phi}$. The solution is usually obtained via an iterative optimization procedure, where S is maximized (or equivalently, the *dissimilarity* is minimized). Such procedures require a good initialization (*i.e.* the

transformation must be close to identity) and are computationally expensive as the evaluation of S requires the actual execution of each intermediate transformation. Furthermore, landmark extraction and correspondence implicitly assumes, that one can observe some image features (*e.g.* gray-level of pixels [15]) f and g that are *covariant* under the transformation

$$f(\mathbf{x}) = g(\phi(\mathbf{x})) = g(\mathbf{y}). \tag{2}$$

However, lack of characteristic features (*e.g.* binary images, printed art) or changes in features (*e.g.* illumination changes, mulimodality) make landmark extraction and matching unreliable in many cases. Segmentation of such images is often straightforward and is available as an intermediate step of a complex image analysis task. Herein, we will discuss a generic correspondence-less framework which works well in such situations.

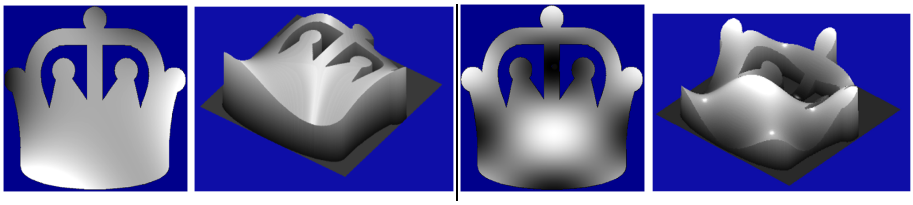

Fig. 1. The effect of applying a polynomial (left) and a trigonometric (right) ω function can be interpreted as a consistent colorization or as a volume

Since correspondences are not available, Eq. (1) cannot be used directly. However, individual point matches can be integrated out yielding the following integral equation:

$$\int_{\mathcal{D}} \mathbf{y} d\mathbf{y} = \int_{\phi(\mathcal{F})} \mathbf{z} d\mathbf{z}, \tag{3}$$

where $\mathcal{D}$ corresponds to the *observation* shape's domain and $\phi(\mathcal{F})$ is the transformed *template* shape's domain. Note that computing the latter integral involves the actual execution of the transformation ϕ on $\mathcal{F}$, which might be computationally unfavorable. Therefore, let us rewrite the above integrals over the *template*'s domain $\mathcal{F}$ and *observation*'s domain $\mathcal{D}$ by making use of the integral transformation $\mathbf{z} \mapsto \phi(\mathbf{x})$ and $d\mathbf{z} \mapsto |J_\phi(\mathbf{x})| d\mathbf{x}$:

$$\int_{\mathcal{D}} \mathbf{y} d\mathbf{y} = \int_{\mathcal{F}} \phi(\mathbf{x}) |J_\phi(\mathbf{x})| d\mathbf{x}, \tag{4}$$

where $|J_\phi(\mathbf{x})|$ is the Jacobian determinant of the transformation ϕ. Note that the above equation corresponds to a system of n equations, where n is the dimension of the shapes. Although the space of allowed deformations is low dimensional, determined by the number of free parameters k of the deformation ϕ, n is typically 2 (planar shapes) or 3 (3D objects), which is not sufficient to solve for all parameters of a real deformation. Therefore we need a general

mechanism to construct new equations. Indeed, Eq. (1) remains valid when a function $\omega : \mathbb{R}^n \to \mathbb{R}$ is acting on both sides of the equation

$$\omega(\mathbf{y}) = \omega(\phi(\mathbf{x})), \tag{5}$$

and the integral equation of Eq. (4) becomes

$$\int_{\mathcal{D}} \omega(\mathbf{y}) d\mathbf{y} = \int_{\mathcal{F}} \omega(\phi(\mathbf{x}))|J_\phi(\mathbf{x})| d\mathbf{x}. \tag{6}$$

Adopting a set of nonlinear functions $\{\omega_i\}_{i=1}^{\ell}$, each ω_i generates a new equation yielding a system of ℓ independent equations. Hence we are able to generate sufficient number of equations by choosing $\ell \geq k$. Intuitively, each ω_i generates a consistent coloring of the shapes and the equations in Eq. (6) match the volume of the applied ω_i function over the shapes (see Fig. 1). The parameters of the aligning transformation ϕ are then simply obtained as the solution of the nonlinear system of equations Eq. (6). In practice, usually an overdetermined system is constructed (*i.e.* $\ell > k$), which is then solved in the *least squares sense* by minimizing the algebraic error. Hereafter, we will omit the integration domains from the equations.

Algorithm 1. Pseudo code of the registration algorithm

Require: *template* and *observation* objects
Ensure: The transformation parameters of ϕ
1: Choose a set of $\ell > k$ nonlinear functions $\{\omega_i\}_{i=1}^{\ell}$.
2: Compute the normalizing transformations which maps coordinates into $[-0.5, 0.5]$.
3: Construct the system of equations.
4: Find a least-squares solution of the system using the *Levenberg-Marquardt* algorithm. Use the identity transformation for initialization.
5: Unnormalizing the solution gives the parameters of the aligning transformation.

What kind of ω functions can be used to generate these independent equations? From a theoretical point of view, only trivial restrictions apply: the functions must be integrable and rich enough (*i.e.* generate a non-constant colorization). Furthermore, they have to be unbiased: each equation should have an equally balanced contribution to the algebraic error, which can be achieved by normalizing the images into the unit square (or cube in 3D) around the origin and the range of the ω functions should also be normalized [10]. From a practical point of view, we have to solve a system of integral equations meaning that intermediate deformations need to be evaluated hence complexity is highly dependent on image size. If we could get rid of the integration in the equations, then considerable speed-up could be achieved. Fortunately, the equation of Eq. (6) can be reduced to a plain polynomial system under the following conditions [5, 10]:

1. The deformation ϕ is given as a linear combination of basis functions. Note that the most common transformation groups, such as linear, polynomial and

thin plate spline deformations are of such form, while other diffeomorphisms can be approximated by their Taylor expansion.
2. The adopted set of nonlinear functions $\{\omega_i\}_{i=1}^{\ell}$ are polynomial.

Let us now briefly overview how to use our framework for various medical applications.

3 Medical Applications

3.1 Fusion of Hip Prosthesis X-Ray Images

Hip replacement [16, 17] is a surgical procedure in which the hip joint is replaced by a prosthetic implant. In the short post-operative time, infection is a major concern. An inflammatory process may cause bone resorption and subsequent loosening or fracture, often requiring revision surgery. In current practice, clinicians assess loosening by inspecting a number of post-operative X-ray images of the patient's hip joint, taken over a period of time. Obviously, such an analysis requires the registration of X-ray images. Even visual inspection can benefit from registration as clinically significant prosthesis movement can be very small.

There are two main challenges in registering hip X-ray images: One is the highly non-linear radiometric distortion [18] which makes any greylevel-based method unstable. Fortunately, the segmentation of the prosthetic implant is quite straightforward [19] so shape registration is a valid alternative here. The second problem is that the true transformation is a projective one which depends also on the position of the implant in 3D space. Indeed, there is a rigid-body transformation in 3D space between the implants, which becomes a projective mapping between the X-ray images. Fortunately, the affine assumption is a good approximation here, as the X-ray images are taken in a well defined *standard position* of the patient's leg. For diagnosis, the area around the implant (especially the bottom part of it) is the most important for the physician. It is where the registration must be the most precise. Based on such an alignment, we can *e.g.* visualize the fused follow-up images for evaluation by an expert (see Fig. 2).

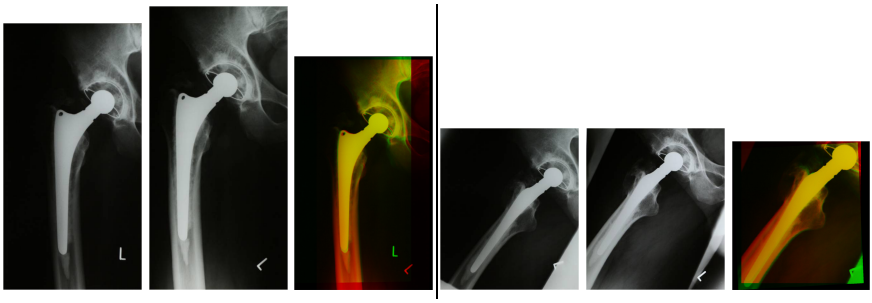

Fig. 2. Fusion of hip prosthesis X-ray image pairs by registering follow up images using a 2D affine transformation (typical CPU time is around 1 sec. in Matlab)

Our framework can be easily applied to register the segmented prosthesis shapes: the diffeomorphism ϕ becomes a non-singular linear transformation matrix $\mathbf{A}$ and the identity relation takes the following simple form:

$$\mathbf{Ax} = \mathbf{y} \quad \Leftrightarrow \quad \mathbf{x} = \mathbf{A}^{-1}\mathbf{y}. \tag{7}$$

Since the Jacobian is the determinant of $\mathbf{A}$, which can be computed as the ratio of the areas of the two planar shapes to be aligned, we can easily construct a system of polynomial equations [5, 6], which is straightforward to solve *e.g.* in Matlab [5] by a classical LSE solver like the *Levenberg-Marquardt* algorithm [7]. Some registration examples can be seen in Fig. 2, where hip prosthesis X-ray image pairs are aligned using a 2D affine transformation. Note that correspondence-based methods are challenged by lack of corner-like landmarks and the nonlinear radiometric distortion between follow-ups. In spite of the inherent modeling error (the physical transformation of the implant is a 3D rigid motion followed by a projection), our method was able to find a precise alignment.

3.2 Registration of Pelvic and Thoracic CT Volumes

The extension of the affine solution to 3D objects [6–8] is relatively straightforward. Typical medical applications include the alignment of pelvic and thoracic CT volumes based on segmented bony structures. Such alignments are important starting points for *e.g.* further elastic alignment of soft tissue organs.

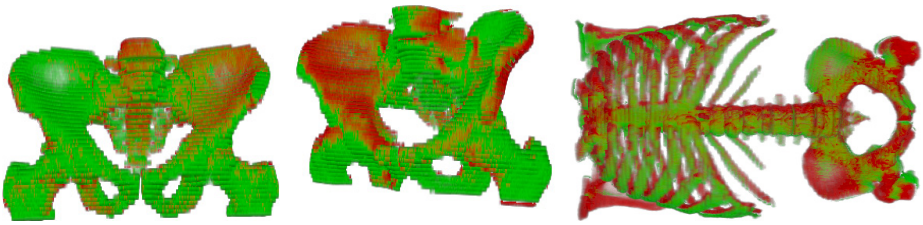

Fig. 3. Superimposed registered 3D bones segmented from CT volumes. Perfect alignment is not possible on the thoracic CT image (last one) due to the relative movements of the bone structure, but affine alignment results are good starting point for *e.g.* lymph node detection.

3.3 Bone Fracture Reduction

Complex bone fracture reduction frequently requires surgical care, especially when angulation or displacement of bone fragments are large. Since the input data is typically a volume CT image, bone fragment repositioning has to be performed in 3D space which requires an expensive special 3D haptic device and quite a lot of manual work. Therefore automatic bone fracture reduction can save considerable time, providing experts with a rough alignment which

can be manually fine-tuned according to anatomic requirements. Since surgical planning involves the biomechanical analysis of the bone with implants, only rigid-body transformations are allowed. In [20], a classical ICP algorithm is used to realign fractures. Winkelbach *et al.* [21] proposed an approach for estimating the relative transformations between fragments of a broken cylindrical structure by using well known surface registration techniques, like 2D depth correlation and the ICP algorithm. In [22], registration is solved by using quadrature filter phase difference to estimate local displacements.

In [9], we formulated the problem as an *affine puzzle*: Given a binary image of an object (the *template*) and another binary image (the *observation*) containing the fragments of the *template*, we want to reconstructs the complete *template* object from its parts. The overall distortion is a global nonlinear transformation with the following constraint [9]:

- the object parts are distinct (*i.e.* either disconnected or separated by segmentation),
- all fragments of the *template* are available, but
- each of them is subject to a different affine deformation, and the partitioning of the *template* object is unknown.

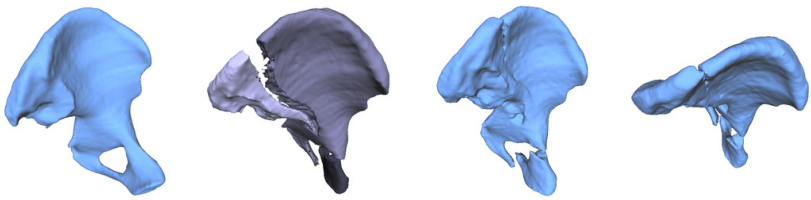

Fig. 4. Bone fracture reduction (CPU time in Matlab was 15 sec. for these 1 megavoxel CT volumes). The *template* is obtained by mirroring the intact bone.

The proposed solution [9] consists in constructing and solving a polynomial system of equations similar to the affine case, which provides all the unknown parameters of the alignment. We have quantitatively evaluated the proposed algorithm on a large synthetic dataset containing 2D and 3D images. The results show that the method performs well and robust against segmentation errors. In Fig. 4, we show a bone fracture reduction solution on a volumetric medical image.

3.4 Elastic Registration of Multimodal Prostate Images

Countries in Europe and USA have been following prostate cancer screening programs since the last 15 years [23]. A patient with abnormal findings is generally advised for a prostate biopsy to diagnose the benign or malignant lesions. During needle biopsy, the most common appearance of malignant lesions in Transrectal Ultrasound (TRUS) is hypoechoic. The accuracy of sonographic finding of

hypoechoic prostate cancer lesions is typically 43% [24]. In contrast, Magnetic Resonance Imaging (MRI) has a negative predictive value of $80\% - 84\%$ for significant cancer and the accuracy of MRI to diagnose prostate cancer is approximately $72\% - 76\%$ [25]. Therefore, MRI may serve as a triage test for men deemed to be at risk of prostate cancer and may reduce the number of re-biopsies while at the same time provide more useful information for those who are sent for biopsy. Consequently, fusion of pre-biopsy MR images onto interoperative TRUS images might increase the overall biopsy accuracy [26].

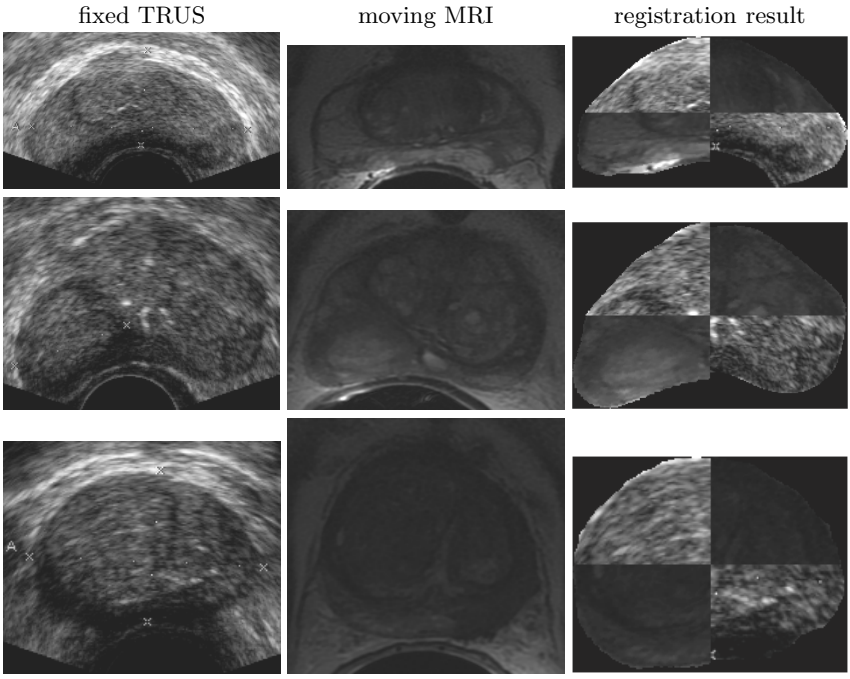

Fig. 5. MRI-TRUST multimodal prostate registration results. Registration result is shown as a checkerborard of TRUS and transformed MR images to show the alignment of the inner structures.

The registration of such prostate images requires a nonlinear deformation model. When ϕ is a nonlinear transformation, then the Jacobian $J_\phi(\mathbf{x})$ is not a constant anymore and thus Eq. (6) has to be used directly:

$$\int \omega_i(\mathbf{y}) d\mathbf{y} = \int \omega_i(\phi(\mathbf{x}))|J_\phi(\mathbf{x})| d\mathbf{x}, \quad i = 1, \ldots, \ell \tag{8}$$

From a practical point of view, this means that our method can be applied to any diffeomorpism ϕ for which one can compute its Jacobian $J_\phi(\mathbf{x})$. Of course, in order to obtain an overdetermined system, ℓ has to be larger than the number

of free parameters of ϕ. In nonlinear medical registration problems, a broadly used class of parametric deformation models are splines, in particular thin plate splines (TPS) [29, 30]. TPS models are quite useful whenever a parametric free-form registration is required but the underlying physical model of the object deformation is unknown or too complex. Given a set of control points $\mathbf{c}_k \in \mathbb{R}^2$ and associated mapping coefficients $a_{ij}, w_{ki} \in \mathbb{R}$ with $i = 1, 2$, $j = 1, 2, 3$ and $k = 1, \ldots, K$, the TPS interpolating points $\mathbf{c}_k$ is given by [30]

$$\varphi_i(\mathbf{x}) = a_{i1}x_1 + a_{i2}x_2 + a_{i3} + \sum_{k=1}^{K} w_{ki} Q(||\mathbf{c}_k - \mathbf{x}||) \;, \tag{9}$$

where $Q : \mathbb{R} \to \mathbb{R}$ is the *radial basis function*

$$Q(r) = r^2 \log r^2 \;.$$

The local parameters are also required to satisfy the following additional constraints [30], meaning basically that the TPS at infinity behaves according to its affine term:

$$\sum_{k=1}^{K} w_{ki} = 0 \quad \text{and} \quad \sum_{k=1}^{K} c_{kj} w_{ki} = 0, \quad i, j = 1, 2 \;. \tag{10}$$

Note that parameters include 6 global affine parameters a_{ij} and $2K$ local coefficients w_{ki} for the control points. In classical correspondence based approaches, control points are placed at extracted point matches, and the deformation at other positions is interpolated by the TPS. When correspondences are available, the exact mapping of the control points are also known which, using Eq. (9), provides constraints on the unknown parameters. Therefore in such cases, a TPS can be regarded as an optimal *interpolating* function whose parameters are usually recovered via a complex optimization procedure [29, 30].

However, we are interested in solving the TPS registration problem without correspondences. Therefore in our approach, a TPS can be considered as a parametric model to *approximate* the underlying deformation field [10]. Control points (*i.e.* radial basis functions) can be placed *e.g.* on a uniform grid in order to capture local deformations everywhere. Obviously, a finer grid would allow a more refined approximation of the deformation field at the price of an increased number of free parameters.

To construct our system of equations Eq. (8), we need the Jacobian $|J_\varphi(\mathbf{x})|$ of the transformation φ, which is composed of the following partial derivatives $(i, j = 1, 2)$ [10]

$$\frac{\partial \varphi_i}{\partial x_j} = a_{ij} - \sum_{k=1}^{K} 2w_{ki}(c_{kj} - x_j)\big(1 + \log(||\mathbf{c}_k - \mathbf{x}||^2)\big) \;. \tag{11}$$

The system is then solved via *Levenberg-Marquardt* algorithm [10].

In [14], we have improved the generic non-linear registration framework of [10] by establishing prostate-specific point correspondences and regularizing the

overall deformation. The point correspondences under the influence of which the thin-plate bends are established on the prostate contours by a method based on matching the shape-context ([2]) representations of contour points using Bhattacharyya distance ([27]). The approximation and regularization of the bending energy of the thin-plate splines are added to the set of non-linear TPS equations and are jointly minimized for a solution. Fig. 5 shows some registration results on multimodal prostate images.

3.5 Elastic Registration of 3D Lung CT Volumes

Lung alignment is a crucial task in lung cancer diagnosis [28]. During the treatment, changes in the tumor size are determined by comparing *follow-up* PET/CT scans which are taken at regular intervals depending on the treatment and the size of the tumor. Due to respiratory motion, the lung is subject to a nonlinear deformation between such *follow-up*s, hence it is hard to automatically find correspondences. A common practice is to determine corresponding regions by hand, but this makes the procedure time consuming and the obtained alignments may not be accurate enough for measuring changes.

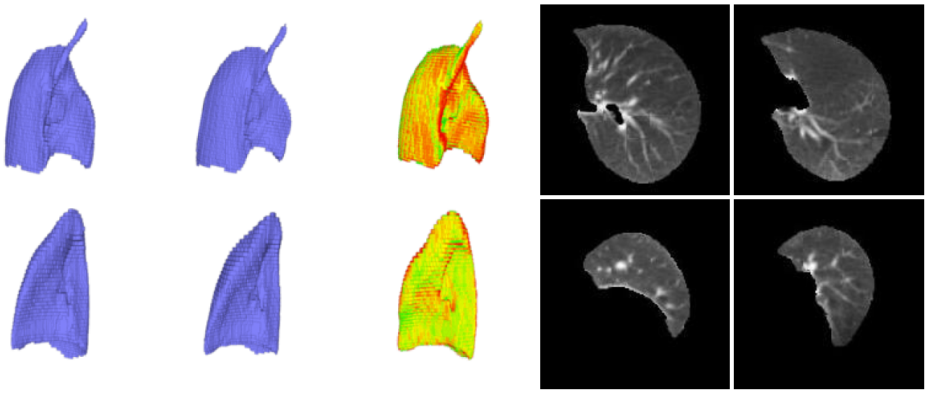

Fig. 6. Alignment of lung CT volumes and the combined slices of the original and the transformed images as an 8x8 checkerboard pattern. Segmented 3D lung images were generated by the *InterView Fusion software of Mediso Ltd.*.

Our algorithm has been successfully applied [11, 12] to align 3D lung CT scans. As usual in elastic medical imaging, the adopted parametric model is a 3D Thin plate splines (TPS) [29, 30] $\varsigma : \mathbb{R}^3 \to \mathbb{R}^3$ which can also be decomposed as three coordinate functions $\varsigma(\mathbf{x}) = [\varsigma_1(\mathbf{x}), \varsigma_2(\mathbf{x}), \varsigma_3(\mathbf{x})]^T$. Given a set of control points $c_k \in \mathbb{R}^3$ and associated mapping coefficients $a_{ij}, w_{ki} \in \mathbb{R}$ with $i = 1, \ldots, 3, j = 1, \ldots, 4$ and $k = 1, \ldots, K$, the TPS functions are

$$\varsigma_i(\mathbf{x}) = a_{i1}x_1 + a_{i2}x_2 + a_{i3}x_3 + a_{i4} + \sum_{k=1}^{K} w_{ki} Q(\|c_k - \mathbf{x}\|) \tag{12}$$

where $Q : \mathbb{R} \to \mathbb{R}$ is the radial basis function, which has the following form in 3D [29]:

$$Q(r) = |r|.$$

The number of the necessary parameters are $N = 3(K+4)$ consisting of 12 affine parameters a_{ij} and 3 coefficients w_{ki} for each of the K control points c_k.

As for the prostate registration problem, we also included a bending energy regularization to ensure the proper alignment of the inner structures. Some registration results are presented in Fig. 6, where we also show the achieved alignment on grayscale slices of the original lung CT images. For these slices, the original and transformed images were combined as an 8×8 checkerboard pattern.

4 Conclusion

A unified framework for correspondence-less registration of 2D and 3D shapes has been presented. The method is applicable for various diffeomorphic deformations. In this paper, we have summarized our earlier results and peresented different medical applications. Demo implementations of our method are also available from `http://www.inf.u-szeged.hu/~kato/software/` as follows:

- *Affine Registration of Planar Shapes*: JAVA code with a direct solver (only runs under Windows).
- *Affine Registration of 3D Objects*: JAVA code with multi-threading ($\approx$ 0.2sec. CPU time for megavoxel volumes).
- *Nonlinear Shape Registration without Correspondences*: Implements planar homography, extension to other nonlinear deformations is relatively easy.

Acknowledgments. This research was partially supported by the grant K75637 of the Hungarian Scientific Research Fund; the grant CNK80370 of the National Innovation Office (NIH) & the Hungarian Scientific Research Fund (OTKA); the European Union and the European Social Fund through project FuturICT.hu (TAMOP-4.2.2.C-11/1/KONV-2012-0013).

The author gratefully acknowledges the contributions of Csaba Domokos, Zsolt Santa, Jozsef Nemeth, and Attila Tanács from University of Szeged, Hungary; Jhimli Mitra, Soumya Ghose, and Fabrice Meriaudeau from Le2i-UMR CNRS 6306, Université de Bourgogne, France.

The fractured bone CT images were obtained from the University of Szeged, Department of Trauma Surgery and were used with permission of Prof. Endre Varga, MD.

Pelvic CT studies and hip prosthesis Xray images were provided by Endre Szabó, Ádám Perényi, Ágnes Séllei and András Palkó from the Radiology Department of the University of Szeged.

Lung CT images were provided by László Papp from Mediso Ltd., Hungary.

References

1. Holden, M.: A review of geometric transformations for nonrigid body registration. IEEE Transactions on Pattern Analysis and Machine Intelligence 27, 111–128 (2008)
2. Belongie, S., Malik, J., Puzicha, J.: Shape matching and object recognition using shape context. IEEE Transactions on Pattern Analysis and Machine Intelligence 24, 509–522 (2002)
3. Heikkilä, J.: Pattern matching with affine moment descriptors. Pattern Recognition 37, 1825–1834 (2004)
4. Hagege, R., Francos, J.M.: Parametric estimation of multi-dimensional affine transformations:an exact linear solution. In: Proceedings of International Conference on Acoustics, Speech, and Signal Processing, Philadelphia, USA, vol. 2, pp. 861–864. IEEE (2005)
5. Domokos, C., Kato, Z.: Parametric estimation of affine deformations of planar shapes. Pattern Recognition 43, 569–578 (2010)
6. Tanács, A., Domokos, C., Sladoje, N., Lindblad, J., Kato, Z.: Recovering Affine Deformations of Fuzzy Shapes. In: Salberg, A.-B., Hardeberg, J.Y., Jenssen, R. (eds.) SCIA 2009. LNCS, vol. 5575, pp. 735–744. Springer, Heidelberg (2009)
7. Tanács, A., Sladoje, N., Lindblad, J., Kato, Z.: Estimation of linear deformations of 3D objects. In: Proceedings of International Conference on Image Processing, Hong Kong, China, pp. 153–156. IEEE (2010)
8. Tanacs, A., Kato, Z.: Fast linear registration of 3D objects segmented from medical images. In: Proceedings of International Conference on BioMedical Engineering and Informatics, Shanghai, China, pp. 299–303. IEEE (2011)
9. Domokos, C., Kato, Z.: Affine Puzzle: Realigning Deformed Object Fragments without Correspondences. In: Daniilidis, K., Maragos, P., Paragios, N. (eds.) ECCV 2010, Part II. LNCS, vol. 6312, pp. 777–790. Springer, Heidelberg (2010)
10. Domokos, C., Nemeth, J., Kato, Z.: Nonlinear shape registration without correspondences. IEEE Transactions on Pattern Analysis and Machine Intelligence 34, 943–958 (2012)
11. Santa, Z., Kato, Z.: Elastic registration of 3D deformable objects. In: Proceedings of International Conference on Digital Image Computing: Techniques and Applications, Fremantle, Australia. IEEE (2012)
12. Santa, Z., Kato, Z.: A unifying framework for non-linear registration of 3D objects. In: Proceedings of International Conference on Cognitive Infocommunications, Kassa, Slovakia, pp. 547–552. IEEE (2012)
13. Rohr, K., Stiehl, H.S., Sprengel, R., Buzug, T.M., Weese, J., Kuhn, M.H.: Landmark-based elastic registration using approximating thin-plate splines. IEEE Transactions on Pattern Analysis and Machine Intelligence 20, 526–534 (2001)
14. Mitra, J., Kato, Z., Marti, R., Oliver, A., Llado, X., Sidibe, D., Ghose, S., Vilanova, J.C., Comet, J., Meriaudeau, F.: A spline-based non-linear diffeomorphism for multimodal prostate registration. Medical Image Analysis 16, 1259–1279 (2012)
15. Hagege, R., Francos, J.M.: Parametric estimation of affine transformations: An exact linear solution. Journal of Mathematical Imaging and Vision 37, 1–16 (2010)
16. Downing, M., Undrill, P., Ashcroft, P., Hukins, D., Hutchison, J.: Automated femoral measurement in total hip replacement radiographs. In: Proceedings of International Conference on Image Processing and Its Applications, Dublin, Ireland, vol. 2, pp. 843–847. IEEE (1997)

17. Hardinge, K., Porter, M.L., Jones, P.R., Hukins, D.W.L., Taylor, C.J.: Measurement of hip prostheses using image analysis. the maxima hip technique. Journal of Bone and Joint Surgery 73-B, 724–728 (1991)
18. Florea, C., Vertan, C., Florea, L.: Logarithmic Model-Based Dynamic Range Enhancement of Hip X-Ray Images. In: Blanc-Talon, J., Philips, W., Popescu, D., Scheunders, P. (eds.) ACIVS 2007. LNCS, vol. 4678, pp. 587–596. Springer, Heidelberg (2007)
19. Oprea, A., Vertan, C.: A quantitative evaluation of the hip prosthesis segmentation quality in x-ray images. In: Proceedings of International Symposium on Signals, Circuits and Systems, Iasi, Romania, vol. 1, pp. 1–4. IEEE (2007)
20. Erdőhelyi, B., Varga, E.: Semi-automatic bone fracture reduction in surgical planning. In: Proceedings of the International Conference on Computer Assisted Radiology and Surgery. International Journal of Computer Assisted Radiology and Surgery, vol. 4, pp. S98–S99. Springer, Berlin (2009)
21. Winkelbach, S., Westphal, R., Goesling, T.: Pose Estimation of Cylindrical Fragments for Semi-automatic Bone Fracture Reduction. In: Michaelis, B., Krell, G. (eds.) DAGM 2003. LNCS, vol. 2781, pp. 566–573. Springer, Heidelberg (2003)
22. Pettersson, J., Knutsson, H., Borga, M.: Non-rigid registration for automatic fracture segmentation. In: Proceedings of International Conference on Image Processing, Atlanta, GA, USA, pp. 1185–1188. IEEE (2006)
23. Andriole, G.L., Crawford, E.D., Grubb, R.L., Buys, S.S., Chia, D., Church, T.R., Fouad, M.N., Gelmann, E.P., Reding, D.J., Weissfeld, J.L., Yokochi, L.A., O'Brien, B., Clapp, J.D., Rathmell, J.M., Riley, T.L., Hayes, R.B., Kramer, B.S., Izmirlian, G., Miller, A.B., Pinsky, P.F., Prorok, P.C., Gohagan, J.K., Berg, C.D.: Mortality results from a randomized prostate-cancer screening trial. The New England Journal of Medicine 360, 1310–1319 (2009)
24. Carroll, P., Shinohara, K.: Transrectal ultrasound guided prostate biopsy. Technical report, Department of Urology, University of California, San Francisco (2010), `http://urology.ucsf.edu/patientGuides.html` (accessed December 30, 2010)
25. Vilanova, J.C., Barceló-Vidal, C., Comet, J., Boada, M., Barceló, J., Ferrer, J., Albanell, J.: Usefulness of prebiopsy multi-functional and morphologic MRI combined with the free-to-total PSA ratio in the detection of prostate cancer. American Journal of Roentgenology 196, W715–W722 (2011)
26. Hu, Y., Ahmed, H.U., Taylor, Z., Allem, C., Emberton, M., Hawkes, D., Barratt, D.: MR to ultrasound registration for image-guided prostate interventions. Medical Image Analysis (2011) (in press), doi:10.1016/j.media.2010.11.003
27. Mitra, J., Srikantha, A., Sidibé, D., Martí, R., Oliver, A., Lladó, X., Vilanova, J.C., Meriaudeau, F.: A shape-based statistical method to retrieve 2D TRUS-MR slice correspondence for prostate biopsy. In: Proc. of SPIE Medical Imaging, San Diego, Calfornia, USA, vol. 8314, pp. 83143M-1–83143M-9 (2012)
28. Bryant, A.S., Cerfolio, R.J.: The maximum standardized uptake values on integrated FDG-PET/CT is useful in differentiating benign from malignant pulmonary nodules. The Annals of Thoracic Surgery 82, 1016–1020 (2006)
29. Bookstein, F.L.: Principal warps: Thin-Plate Splines and the Decomposition of deformations. IEEE Transactions on Pattern Analyis and Machine Intelligence 11, 567–585 (1989)
30. Zagorchev, L., Goshtasby, A.: A comparative study of transformation functions for nonrigid image registration. IEEE Transactions on Image Processing 15, 529–538 (2006)